

# Synthesis of YAP nanopowder by a soft chemistry route

J.F. Carvalho<sup>a,b,\*</sup>, F.S. De Vicente<sup>a,c</sup>, S. Pairis<sup>a</sup>, P. Odier<sup>a</sup>,  
A.C. Hernandez<sup>c</sup>, A. Ibanez<sup>a</sup>

<sup>a</sup> Institut Néel, CNRS and Université J. Fourier, 25 Avenue des Martyrs BP 166, 38042, Grenoble, France

<sup>b</sup> Instituto de Física, Universidade Federal de Goiás - CP 161, 74001-970, Goiânia - GO, Brazil

<sup>c</sup> Instituto de Física de São Carlos, Universidade de São Paulo, CP 369, 13560-970 São Carlos - SP, Brazil

Received 23 January 2009; received in revised form 10 March 2009; accepted 12 March 2009

Available online 10 April 2009

## Abstract

Polycrystalline fine powder of  $\text{YAlO}_3$  (YAP) was synthesized by the modified polymeric precursor method. A preliminary gradual pyrolytic decomposition under nitrogen flux was crucial in the removal process of organic residues to avoid the formation of molecular level inhomogeneities. YAP single phase was crystallized at temperatures between 950 °C and 1000 °C using chemically homogeneous ball-milled amorphous particles and very fast heating rates, corresponding to the lowest synthesis temperature of pure YAP nanopowder by soft chemistry routes.

© 2009 Elsevier Ltd. All rights reserved.

**Keywords:** Powders-chemical preparation;  $\text{YAlO}_3$  (YAP)

## 1. Introduction

YAP ( $\text{YAlO}_3$ ) doped with rare earth or transition metals demonstrate very attractive properties being a promising material as a host matrix for laser,<sup>1</sup> phosphors,<sup>2</sup> scintillator,<sup>3</sup> thermoluminescent detector,<sup>4</sup> holographic recording medium<sup>5</sup> and pigments.<sup>6</sup> YAP is one of four crystalline phases occurring in the system  $\text{Al}_2\text{O}_3$ – $\text{Y}_2\text{O}_3$ <sup>7,8</sup> presenting an orthorhombic perovskite structure with Y/Al ratio 1:1. Other three phases in that system are a cubic garnet structure with Al-richer composition,  $\text{Y}_3\text{Al}_5\text{O}_{12}$  (YAG), a monoclinic Y-richer phase,  $\text{Y}_4\text{Al}_2\text{O}_9$  (YAM), and a metastable hexagonal phase (YAH) with the same YAP stoichiometry normally appearing during the synthesis of YAG and YAP by soft chemistry routes.<sup>8</sup>

Synthesis of YAP powder has been performed by solid-state reaction synthesis,<sup>7</sup> sol–gel,<sup>9</sup> modified polymeric precursor method<sup>10</sup> and a more complex method used by Mathur et al.<sup>11</sup> who obtained pure YAP through the intermediate synthesis of a bimetallic alkoxide of Y and Al. Solid-state reactions synthe-

sis of YAP requires very high temperatures, above 1500 °C.<sup>7</sup> Synthesis by chemical routes presents some important difficulties related to problems in controlling chemical homogeneity at a molecular level which combined with the existence of many phases of the  $\text{Al}_2\text{O}_3$ – $\text{Y}_2\text{O}_3$  system impose limits to the reduction of the synthesis temperature or require more complex and expensive methods for the synthesis of YAP single phase. We propose a new route based on the modified polymeric precursor method, carefully controlling oxidation of the organic precursors to overcome all the chemical inhomogeneity problems. Control of all the mineralization process allows preparing pure YAP nanopowders at significantly lower temperatures than those previously involved for the polymeric precursor synthesis.

## 2. Experimental

The metal precursors used in this study were yttrium nitrate ( $\text{Y}(\text{NO}_3)_3 \cdot 6\text{H}_2\text{O}$ , 99.9%, Strem Chemicals) and aluminum nitrate ( $\text{Al}(\text{NO}_3)_3 \cdot 9\text{H}_2\text{O}$ ,  $\geq 98.5\%$ , Riedel-de Haen). As these nitrates are highly hygroscopic, special care was taken during weighing to ensure accurate starting stoichiometry. The compounds were previously dried in low vacuum and maintained in a dry glove box where they were weighed. Yttrium and aluminum nitrates in 1:1 molar ratio were then dissolved in deionized water at 80 °C, followed by the addition of citric

\* Corresponding author at: Instituto de Física, Universidade Federal de Goiás - CP 161, 74001-970, Goiânia - GO, Brazil. Tel.: +55 62 3521 1122; fax: +55 62 3521 1122.

E-mail addresses: [jesiel.carvalho@pq.cnpq.br](mailto:jesiel.carvalho@pq.cnpq.br), [carvalho@if.ufg.br](mailto:carvalho@if.ufg.br) (J.F. Carvalho).

acid (99%, Sigma–Aldrich) with the metal (Y, Al) to the citric acid molar ratio set at 1:3. After the complete dissolution of these starting compounds, D-Sorbitol (98%, Sigma–Aldrich) was added to promote the polyesterification reactions between Y and Al citrates. The molar ratio of citric acid to sorbitol was 3:2. A clear solution was obtained after a few minutes at pH 1.6 and an overnight heating at the same temperature of 80 °C led to a homogeneous viscous resin, after about 70% water evaporation, with slight yellow coloration and long stability over several months. Vigorous magnetic stirring assisted all of the process. In this work the resin was first dried under N<sub>2</sub> flux at 250 °C using a heating rate of 0.5 °C/min to avoid uncontrolled combustions inducing hot spots and the consequent formation of chemical inhomogeneities. This drying procedure yielded a soft and porous dark brown solid that was easily crushed in agate mortar to produce a fine and homogeneous amorphous powder, in this work designated as the *primary precursor*.

Two different thermal treatments were then used to remove the organic components of the primary precursor powder during the mineralization process. First, a calcination route consisting of an annealing at 400 °C for 24 h to remove the major organic fractions followed by another one at 700 °C/24 h to complete the removal of organics and consolidate the formation of the amorphous network. A second pyrolytic route, where the decomposition of organics take place under N<sub>2</sub> atmosphere at 700 °C for 24 h. The first calcination treatment resulted in an amorphous white powder, here designated as the *calcinated amorphous precursor*, while the second pyrolytic process produced a black amorphous powder, the so-called *pyrolytic amorphous precursor*. Fig. 1 shows the different stages for the synthesis of both amorphous YAP precursors obtained through the calcination and pyrolysis treatments.

To improve the homogeneity and reactivity of these amorphous powders, they were ball milled using yttria-stabilized zirconia spheres (YSZ, Tosoh Co.). The process was accomplished in a homemade ball milling system. The best ball milling results were obtained from a two-stage process. The first one consisted of a dry ball milling for about 72 h using 5 mm YSZ balls, while for the second ball milling cycle of around 12 h, acetone was added. The crushing was more efficient in a dry medium due to high attrition mechanisms, but the second wet stage was also important to favor the powder recovery. The ball-milled powder was ultrasonically processed using acetone as liquid medium and this deflocculated suspension was left to rest for 5 min to decant the larger particles at the bottom of the beaker. The remaining suspension was then separated and dried at 80 °C. By this procedure, fine amorphous powders with particle diameters ranging between 100 nm and 300 nm were obtained.

Phase analysis was carried out by X-ray powder diffraction (XRD) technique using the Co K $\alpha$  radiation of a Siemens D5000 diffractometer. Scanning electron micrographs (SEM) were recorded with a Jeol 940A electron microscope. Coupled differential thermal analysis and thermogravimetry (DTA–TG) were carried out in a Setaram (TAG 1600) equipment using alumina crucibles.

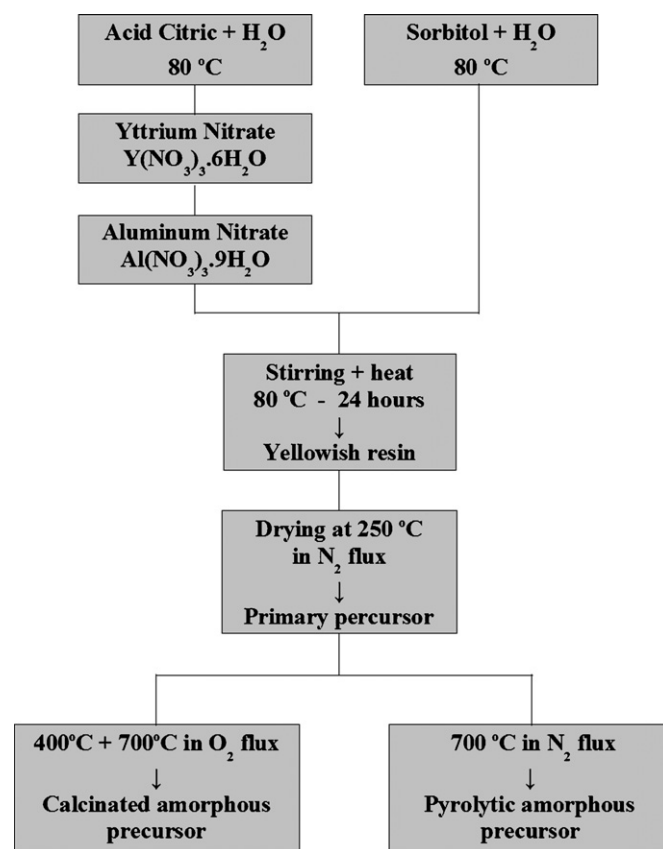


Fig. 1. Diagram with the sequence steps used for the synthesis of the amorphous precursor of YAP.

### 3. Results and discussion

#### 3.1. YAP synthesis from calcinated amorphous powder

The production of the amorphous precursor powder by the calcination route, under oxygen atmosphere, usually leads to the formation of large aggregates like that shown in Fig. 2 by scanning electron microscopy (SEM) with around 20  $\mu$ m in the

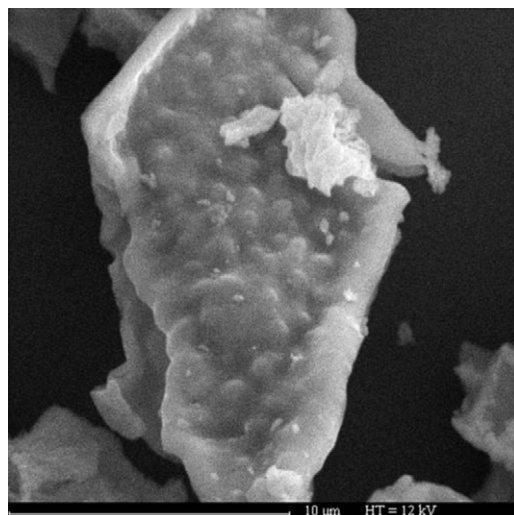


Fig. 2. Large aggregates of amorphous powder prepared by the calcination route.

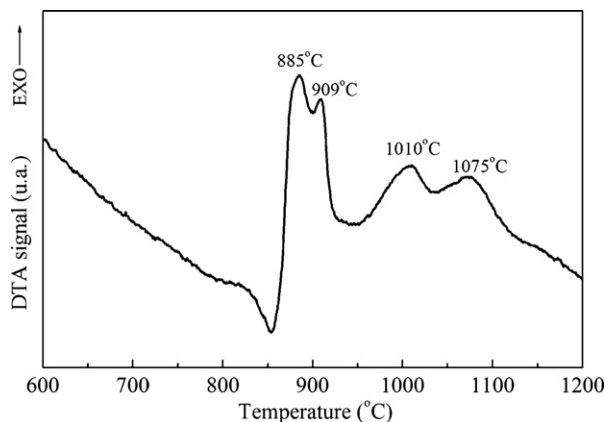


Fig. 3. DTA curve of calcinated amorphous precursor powder recorded under air with a heating rate of 5 °C/min.

longitudinal direction. This strong aggregation can be associated to the intense combustion of organics with high O<sub>2</sub> content, thus resulting in the typical problem of hot spots. The first critical stage, from the point of view of the chemical homogeneity and formation of aggregates, is the resin drying process. The rapid heating of the resin to temperatures of around 300 °C leads to the formation of hot spots due to localized strong combustions associated to non-uniform solvent evaporation, hence producing macroscopic heterogeneities in the dried powder. Additionally, in the subsequent calcinations chemical inhomogeneities can also be generated as a consequence of fast firing.

Chemical inhomogeneities of amorphous precursor can favor the formation of the intermediate YAG and YAM stable phases during the synthesis of crystalline powder. This process intensifies with the use of large amorphous precursor particles and low heating rates due to the differences in the Al and Y ions mobility.<sup>12</sup> Fig. 3 shows the DTA curve of the calcinated amorphous precursor, using a heating rate of 5 °C/min, which exhibits four exothermic peaks at 885 °C, 909 °C, 1010 °C and 1075 °C corresponding, respectively, to the crystallization of YAM, YAH, YAG and YAP phases as specified by their XRD patterns. If the intermediate stable phases are formed, the pure YAP phase can still be obtained, but in this case requiring the transformation of YAM and YAG into YAP according to the reaction:  $Y_4Al_2O_9$  (YAM) +  $Y_3Al_5O_{12}$  (YAG) → 7  $YAlO_3$  (YAP). However, this reaction requires high energy to overcome diffusional and energetic barriers, like in the conventional solid-state reaction synthesis, and therefore, high temperature values are necessary to complete the reaction, over 1500 °C.<sup>7</sup>

Thus, intending to reduce the synthesis temperature, the entire organic residues removal process must be carefully accomplished, in such a way as to avoid the occurrence of uncontrolled combustion that leads to the formation of large aggregates and to inhomogeneous distribution of metal ions in the amorphous network. On the other hand, ball milling of amorphous precursor combined with very fast heating rates can minimize the generation of inhomogeneities during the crystallization stage. The advantages of this procedure are associated to the reduction of heat and mass diffusion length. In this work, high heating rates were achieved by placing the samples into the previously

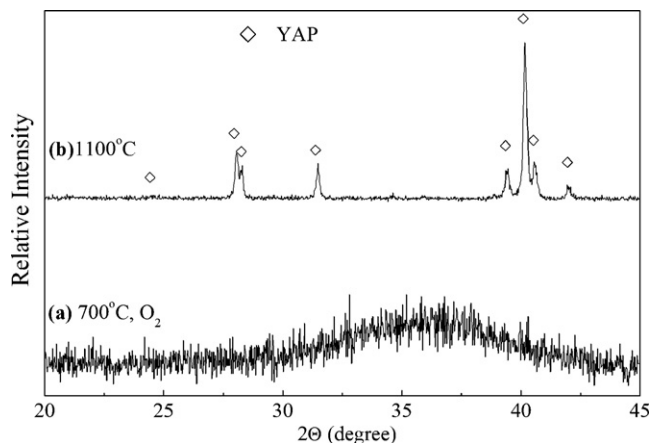


Fig. 4. XRD results obtained for the ball-milled calcinated powder. Pure YAP was obtained at 1100 °C using a fast heating treatment.

heated furnace at the final synthesis temperature, here designated as *fast heating*. Fig. 4(a) shows X-ray measurements of the amorphous powder calcinated at 700 °C in O<sub>2</sub> flux, where no crystalline phase was detected. Fig. 4(b) presents the X-ray profile of pure YAP phase prepared from a ball-milled amorphous precursor with particle size in the range of 200–300 nm and using fast heating at 1100 °C for 3 h. This synthesis temperature was the lowest one that resulted in single YAP phase by this calcination route.

### 3.2. YAP synthesis through the pyrolysis route

In this case, the direct combustion under oxygen atmosphere of the primary precursor powder was replaced by a gradual pyrolytic decomposition under nitrogen flux at 700 °C. By this method, we intended to improve the chemical homogeneity of the amorphous precursor by avoiding possible non-uniform decomposition during the firing procedure.

The DTA curve of the pyrolytic amorphous powder obtained at 700 °C in N<sub>2</sub> flux is shown in Fig. 5 (solid line). It exhibits a very different behavior from the calcinated one measured with

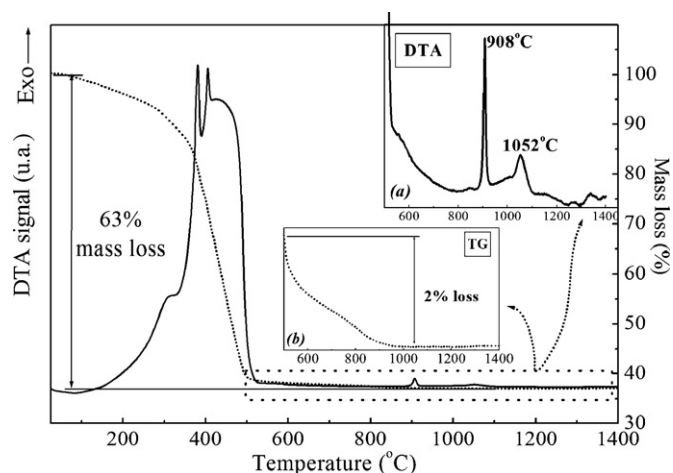


Fig. 5. DTA–TG of the pyrolytic amorphous powder obtained at 700 °C using a heating rate of 5 °C/min and a gas flux consisting of 80% Ar + 20% O<sub>2</sub>.



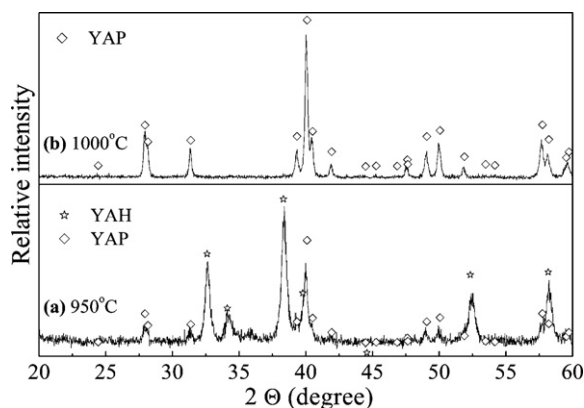


Fig. 6. Evolution of YAP phase formation using ball-milled pyrolytic amorphous precursor and fast heating process.

the same heating rate, Fig. 3, where four consecutive peaks are observed between 850 °C and 1150 °C, which corresponds to the formation of YAM, YAH, YAG and YAP phases. In fact, this DTA of the pyrolytic powder, in addition to the complex band between 200 °C and 500 °C related to the oxidation of pyrolytic carbon and other organic residues, shows only two main exothermic peaks, insert (a) of Fig. 5, corresponding to the powder crystallization. These two peaks, centered at 908 °C and 1052 °C, are related to the formation of crystalline metastable YAH and to the YAH–YAP structural transition, respectively. Concerning this DTA curve, it is difficult to point out other weak exothermic peaks from the baseline and to specify their corresponding temperatures, confirming in all cases that the formation of the intermediates YAM and YAG phases is negligible for the pyrolysis route.

On the other hand, the insert (b) of Fig. 5 shows that the mass loss associated to the crystallization of the previously pyrolyzed powder is just 2 wt%, less than the 5 wt% loss previously observed for a directly calcinated powder (not shown here). This significantly lower mass loss suggests that the intermediate pyrolytic route favors a gradual decomposition of the organic compounds through a better controlled oxidation, hence leading to a more homogeneous amorphous network than that previously obtained by a one-step calcination. This favors the powder crystallization of pure YAP phase, in agreement with the XRD results.

Fig. 6 shows the evolution of the crystalline phase formation from pyrolytic amorphous powders by fast annealings between 950 °C and 1000 °C. Fig. 6(a) shows the X-ray pattern of a ball-milled pyrolytic amorphous precursor annealed at 950 °C for 3 h. YAP and metastable YAH phases were observed, with YAH as the major one. The absence of YAM and YAG phases is a clear indication of the high homogeneity at the molecular level of the pyrolytic amorphous precursor and the wide diffraction peak linewidths suggest an incomplete crystallization. Fig. 6(b) shows the XRD pattern of the single phase YAP crystallized at 1000 °C for 3 h involving the same precursor powder. This is the lowest synthesis temperature of YAP from the polymeric precursor method.

This significant synthesis improvement, through the pyrolysis process that allows the preparation of reactive YAP fine powders

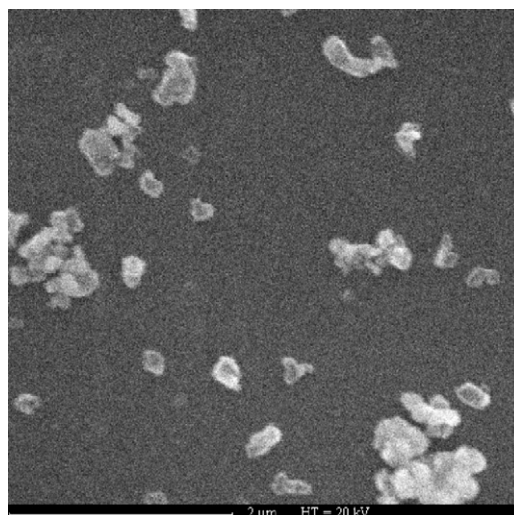


Fig. 7. Scanning electron microscopy of YAP particles.

at low temperatures, is crucial for the in progress preparation of ceramics by sintering. Fig. 7 shows the resulting YAP nanopowder obtained at 1000 °C observed by SEM and shows particle diameters ranging between 100 nm and 300 nm, without any significant uncontrolled sintering, which is necessary for the future preparation of dense ceramics.

#### 4. Conclusions

We have demonstrated that using this modified polymeric precursor method with a carefully controlled mineralization process, it is possible to prepare fine powders of pure YAP phase at temperatures as low as 1000 °C. This is the lowest temperature of YAP synthesis by the polymeric precursor method. We have shown that the process of YAP phase formation is highly dependent of the synthesis route and its formation at low temperatures requires fully avoiding the formation of intermediate stable phases YAM and YAG. This was possible by using a combined pyrolysis and calcination process to avoid uncontrolled decomposition. In addition, combining very fast heating rates during crystallization and ball milling of the amorphous precursor powder allows overcoming time dependent heat and mass diffusional processes that are dominant in the generation of molecular level inhomogeneities. The pyrolysis decomposition route involved in this work can be proposed as a generic method of mineralization to be applied in the preparation of all the wet chemical routes involving organic precursors.

#### Acknowledgements

CAPES/COFECUB Brazil–France cooperation program (project 455/04/06) and CNPq.

#### References

- Romero, J. J., Montoya, E., Bausá, L. E., Agulló-Rueda, F., Andreetta, M. R. B. and Hernandes, A. C., Multiwavelength laser action of Nd<sup>3+</sup>:YAlO<sub>3</sub> single crystals grown by the laser heated pedestal growth method. *Optical Materials*, 2004, **24**, 643–650.

2. Gao, H. and Wang, Y., Photoluminescence of  $\text{Eu}^{3+}$  activated  $\text{YAlO}_3$  under UV–VUV excitation. *Materials Research Bulletin*, 2007, **42**, 921–927.
3. Nikl, M., Yoshikawa, A., Vedda, A. and Fukuda, T., Development of novel scintillator crystals. *Journal of Crystal Growth*, 2006, **292**, 416–421.
4. Zhdachevskii, Ya., Durygin, A., Suchocki, A., Matkovskii, A., Sugak, D., Bilski, P. et al., Mn-doped  $\text{YAlO}_3$  crystal: a new potential TLD phosphor. *Nuclear Instruments and Methods in Physics Research*, 2005, **B227**, 545–550.
5. Loutts, G. B., Warren, M., Taylor, L., Rakhimov, R. R., Ries, H. R., Miller III, G. et al., Manganese-doped yttrium orthoaluminate: a potential material for holographic recording and data storage. *Physical Review*, 1998, **B57**, 3706–3709.
6. Shirpour, M., Faghihi Sani, M. A. and Mirhabibi, A., Synthesis and study of a new class of red pigments based on perovskite  $\text{YAlO}_3$  structure. *Ceramics International*, 2007, **33**, 1427–1433.
7. Medraj, M., Hammond, R., Parvez, M. A., Drew, R. A. L. and Thompson, W. T., High temperature neutron diffraction study of the  $\text{Al}_2\text{O}_3$ – $\text{Y}_2\text{O}_3$  system. *Journal of the European Ceramic Society*, 2006, **26**, 3515–3524.
8. Sim, S.-M., Keller, K. A. and Mah, T.-I., Phase formation in yttrium aluminum garnet powders synthesized by chemical methods. *Journal of Materials Science*, 2000, **35**, 713–717.
9. Tanner, P. A., Law, P.-T., Wong, K.-L. and Fu, L., Preformed sol–gel synthesis and characterization of  $\text{YAlO}_3$ . *Journal of Materials Science*, 2003, **38**, 4857–4861.
10. Harada, M. and Goto, M., Synthesis of Y–Al–O compounds by a polymer complex method. *Journal of Alloys and Compounds*, 2006, **408**, 1193–1195.
11. Mathur, S., Shen, H., Rapalaviciute, R., Kareiva, A. and Donia, N., Kinetically controlled synthesis of metastable  $\text{YAlO}_3$  through molecular level design. *Journal of Materials Chemistry*, 2004, **14**, 3259–3265.
12. MacKenzie, K. J. D. and Kemmitt, T., Evolution of crystalline aluminates from hybrid gel-derived precursors studied by XRD and multinuclear solid-state MAS NMR. II. Yttrium–aluminium garnet,  $\text{Y}_3\text{Al}_5\text{O}_{12}$ . *Thermochimica Acta*, 1999, **325**, 13–18.